Journal of Biotechnology 281 (2018) 150–160

Contents lists available at ScienceDirect

Journal of Biotechnology

journal homepage: www.elsevier.com/locate/jbiotec

Optimisation of enzyme cascades for chiral amino alcohol synthesis in aid of host cell integration using a statistical experimental design approach

Maria F. Villegas-Torres[a,b], John M. Ward[b], Frank Baganz[b,*]

[a] Chemistry Department, Universidad Icesi, Calle 18 No. 122 – 135 Pance, Cali, Colombia
[b] The Advanced Centre for Biochemical Engineering, Department of Biochemical Engineering, Gordon Street, WC1H 0AH, United Kingdom

ARTICLE INFO

Keywords:
Recycling cascade
Sequential pathway
Statistical experimental design
Chiral amino alcohol

ABSTRACT

Chiral amino alcohols are compounds of pharmaceutical interest as they are building blocks of sphingolipids, antibiotics, and antiviral glycosidase inhibitors. Due to the challenges of chemical synthesis we recently developed two TK-TAm reaction cascades using natural and low cost feedstocks as substrates: a recycling cascade comprising of 2 enzymes and a sequential 3-step enzyme cascade yielding 30% and 1% conversion, respectively. In order to improve the conversion yield and aid the future host strain engineering for whole cell biocatalysis, we used a combination of microscale experiments and statistical experimental design. For this we implemented a full factorial design to optimise pH, temperature and buffer type, followed by the application of Response Surface Methodology for the optimisation of substrates and enzymes concentrations. Using purified enzymes we achieved 60% conversion for the recycling cascade and 3-fold improvement using the sequential pathway. Based on the results, limiting steps and individual requirements for host cell metabolic integration were identified expanding the understanding of the cascades without implementing extensive optimisation modelling. Therefore, the approach described here is well suited for optimising reaction conditions as well as defining the relative enzyme expression levels required for construction of microbial cell factories.

1. Introduction

Metabolic engineering is employed in the modification of metabolic networks for the sustainable synthesis of chemicals of industrial interest at lower costs from waste material or natural feedstocks (Yang et al., 1998; Prather and Martin, 2008; Morales et al., 2016). It has been widely implemented over the last 30 years by combining existing pathways, engineering them or developing new ones beyond the host's metabolic boundaries (Prather and Martin, 2008). For example, tetrahydrobiopterin was biosynthesised by cloning the mammalian metabolic pathway in *Escherichia coli* (Yamamoto et al., 2003); isopropanol was produced by identifying homologous enzymes with higher activity following the natural pathway (Hanai et al., 2007); and 1,2,4-butanetriol was synthesised employing a *de novo* pathway approach, in which individual enzymes are identified and coupled for the synthesis of non-natural compounds (Niu et al., 2003). Among the above methodologies the latest is of particular interest as it exponentially expands the chemical repertoire to be biochemically synthesized.

For *de novo* pathway integration there are several challenges that need to be overcome in order to expand its industrial application. Amongst them are: 1) the inherent incompatibility between enzymes within the pathway in terms of reaction conditions (Prather and Martin, 2008); 2) the presence of thermodynamic or kinetic barriers; and 3) the overlap between the new pathway and the cell metabolism (Erb et al., 2017)

Enzymatic kinetic modelling is often used to define reaction mechanism, reactor design, and operational analysis based on optimum yield, productivity, selectivity, space-time-yield and operating conditions (Chen et al., 2007; Gyamerah and Willetts, 1997; Vasic-Racki et al., 2003). In order to develop a particular model initial reaction rates and kinetic constants of all reactions involved must be determined, followed by mathematical formulation of reaction rates and experimental verification of the model. The above requires extensive experimental work to characterise the enzymes in terms of K_m (Michaelis-Menten constant), v_m (maximum velocity) and K_i (inhibitory constant) and to identify the impact of the process conditions (pH, temperature) on the enzyme, and substrates and products stability (Chen et al., 2007; Vasic-Racki et al., 2003). In addition to the extensive experimental work required in this approach, it has been shown that individual reactions do not behave equally when combined and if pure enzymes are employed, then a compatibility assessment with the intrinsic metabolism of the host cell must be performed prior to *in vivo* development

* Corresponding author.
E-mail addresses: mfvillegas@icesi.edu.co (M.F. Villegas-Torres), j.ward@ucl.ac.uk (J.M. Ward), f.baganz@ucl.ac.uk (F. Baganz).

https://doi.org/10.1016/j.jbiotec.2018.07.014
Received 21 February 2018; Received in revised form 6 July 2018; Accepted 9 July 2018

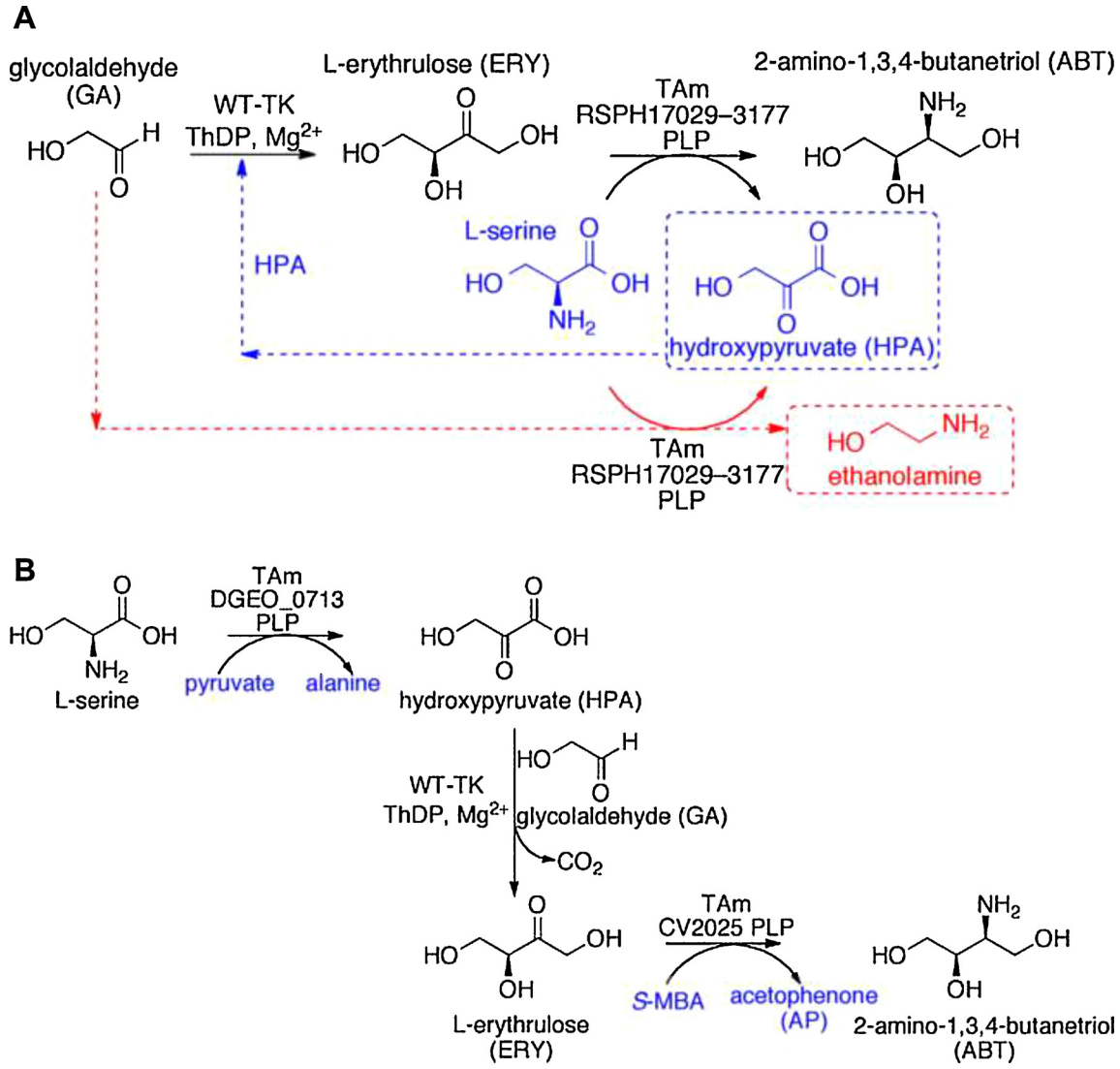

Fig. 1. Reaction schemes employed for the synthesis of 2-amino-1,3,4-butanetriol (ABT) (Villegas-Torres et al., 2015). (a) Recycling *de novo* pathway: an ω-transaminase (RSPH17029-3177) aminates erythrulose using serine as amino donor for the synthesis of ABT and hydroxy pyruvate (HPA); followed by the synthesis of erythrulose (ERY) from glycolaldehyde (GA) and HPA, previously synthesised, employing a transketolase enzyme as biocatalyst. (b) Sequential cascade: first, an α-transaminase (DGEO0713) aminates pyruvate with serine as amino donor, producing alanine and HPA; followed by, a transketolase enzyme which uses the HPA synthesised and GA as substrates for the synthesis of ERY and the release of CO_2; and finally, an ω-transaminase (CV2025) aminates the formed ERY with methylbenzylamine (MBA), synthesising ABT and acetophenone.

(Erb et al., 2017).

At UCL we designed a *de novo* pathway coupling a transaminase with a transketolase enzyme for the synthesis of 2-amino-1,3,4-butanetriol (ABT) (Chen et al., 2006; Ingram et al., 2007; Rios-Solis et al., 2011; Smith et al., 2010), a chiral amino alcohol. These molecules are building blocks of several pharmaceutical and chemical compounds normally synthesised by expensive chemical methods (Contestabile and John, 1996). We employed, a one-pot *in vivo* approach using glycolaldehyde (GA) and β-hydroxypyruvate (HPA) as initial substrates for the transketolase step, followed by a transamination using erythrulose (transketolase product) and isopropylamine (IPA) as substrates. We achieved an 87% conversion supplementing all the substrates involved, namely GA, HPA and IPA (Rios-Solis et al., 2011). In order to avoid substrate supplementation and achieve a full metabolic integration with *E. coli* metabolism as final aim, we initially developed alternative cascades employing a transaminase/transketolase recycling cascade (Fig. 1a) or a sequential three-step pathway (Fig. 1b) with two transaminases and one transketolase enzyme to supply the required HPA from L-serine. Based on the results obtained the recycling cascade (Fig. 1a) was shown to be more efficient than the sequential pathway (Fig. 1b) with 30% conversion yield compared to only 1%, respectively. Considering that the recycling cascade only requires the heterologous expression of two enzymes and less side products remain within the host cell, this system appears to be more advantageous for host metabolic integration (Villegas-Torres et al., 2015). In spite of the above, final conversion must be increased ensuring functional compatibility among the enzymes and thermodynamic and/or kinetic barriers must be identified prior to a full metabolic integration of the *de novo* pathway with the host metabolism (Yang et al., 1998).

Several studies have shown that *E. coli* transketolase enzyme is highly active in different reaction conditions (Bongs et al., 1997; Brocklebank et al., 1999; Cázares et al., 2010; Costelloe et al., 2007; Hibbert et al., 2008, 2007; Martinez-Torres et al., 2007; Mitra et al., 1998; Sprenger et al., 1995); and various transaminases from different organisms have been characterised showing different substrate affinities, as well as diverse optimum reaction conditions (Kaulmann et al., 2007; Kim, 1964; Shin and Kim, 1999; Yonaha and Toyama, 1980). Additionally an effect from the substrates on the pH of the reactions

have been reported, possibly caused by the difference in pKa of the substrates as it might affect a proton shift during the reaction. Therefore, optimum reaction conditions not only depend on the enzymes employed but also on the substrates (Shin and Kim, 1999).

Various biocatalytic studies have employed Response Surface Methodology (RSM) to optimise reactions conditions (Hari Krishna et al., 2000; Zhang et al., 2016; Fang et al., 2016; Babaki et al., 2017) and to determine kinetic constants (Andersson and Adlercreutz, 1999; Beg et al., 2002), because it defines the relationships between independent variables based on dependent responses. According to Baş and Boyacı (2007) RSM implementation in kinetic studies is highly limited because of the diversity of enzymes behaviour, which cannot always be fitted to a second-order polynomial model. In contrast, for optimisation studies this is an excellent approach as long as RSM limitations are taken into account.

As previously mentioned, the overall aim of this work was to increase the conversion from the enzymatic cascades previously reported (Fig. 1) and to identify thermodynamic and/or kinetic barriers for their future host metabolic integration. Due to the extensive experimental work required for kinetic modelling optimisation and the successful implementation of RSM in multi-step biocatalytic optimisation (Fang et al., 2016), we applied RSM to optimise the coupled reactions and identify barriers for host integration. Independent variables and their limits were defined based on the kinetic constants of the main reactions involved in each cascade, and the intrinsic limitations of the systems and those given by their future host. The above, avoids the whole kinetic characterisation of the reactions under various process conditions and simultaneously evaluates functional compatibility among enzymes and the presence of intrinsic thermodynamic and/or kinetic barriers by the experimental evaluation of the cascades as a whole and not in a stepwise approach.

2. Materials and methods

2.1. Strains and plasmids

Transaminases from *Chromobacterium violaceum* (CV2025); *Deinococcus geothermalis* (DGEO0713); *Rhodobacter sphaeroides* (RSPH17029-3177), were expressed in *E. coli* BL21-Gold (DE3) (Agilent Technologies, CA#230132) containing the plasmids pQR801 (Kaulmann et al., 2007), pQR977 and pQR1021 (Villegas-Torres et al., 2015), respectively. *E. coli* transketolase enzyme was over expressed in *E. coli* XL10-Gold (Stratagene, CA#200314) containing the plasmid pQR791 (Martinez-Torres et al., 2007).

2.2. Growth media, culture conditions and enzyme purification

Glycerol stocks of all cultures were stored at −80 °C in 2XYT broth (16 g/ l tryptone, 10 g/ l yeast extract, 5 g/ l NaCl) containing 20% glycerol. Overnight cultures were prepared in 2XYT broth supplemented with appropriate antibiotics. Cells were subcultured using 1% v/v inoculum in 2 l shake flasks containing 500 ml of the same supplemented broth at 37 °C and 250 rpm. Transaminases were induced with 1 mM of IPTG when growing in early exponential phase (OD600 = 0.7), and temperature was dropped to 30 °C until harvesting. Cells were harvested by centrifugation at 13,000 rpm and 4 °C after 5 h of induction, and stored at −20 °C. 15 min before harvesting pyridoxal-5′-phosphate (PLP) was added to the cells expressing the transaminases at a final concentration of 400 μM to improve enzyme activity. Transketolase enzyme was constitutively expressed, thus following the inoculation procedure described above, cells were harvested as described above after 8 h growth without cofactor supplementation at 37 °C and 250 rpm, and stored at −20 °C.

Cell pellets were resuspended in buffer according to the reaction at a 1:25 vol ratio (1 ml of the resuspension buffer per 25 ml of cell suspension), and sonicated (Soniprep 150 sonicator, MSE Sanyo Japan) on ice using 10 cycles of 10 s ON, 10 s OFF at 10%. The sonicated suspension was centrifuged at 13,000 rpm and 4 °C for 60 min. Purification was carried out by nickel affinity using His-Select® Nickel Affinity Gel (Sigma-Aldrich, CA#P6611), following manufacturer recommendations. 250 mM of imidazole was added to the elution buffer and was removed using PD-10 columns (General Electric, CA#17085101) with the reaction buffer. Bradford reagent (Sigma-Aldrich, CA#B6916) was used for total protein concentration quantification (Bradford, 1976) with bovine serum albumin (BSA) (Sigma-Aldrich, CA#A4612) as standard. Enzyme purity was confirmed by SDS-PAGE using 12% Tris-Glycine Precast Gels (Invitrogen, CA#XP00122BOX). All the above buffers were supplemented with 400 μM PLP when working with the transaminases to increase enzyme activity.

2.3. Enzyme reactions

Commercially available substrates were purchased from Sigma-Aldrich (unless otherwise stated). ABT was chemically synthesised following the method by Dequeker et al. (1995) and Ingram et al., (2007). The 1,2-acetonide benzylamine diastereomeric intermediates were separated by silica flash column chromatography (particle size 40–63 μm) to give the (2R-3S)-ABT after subsequent deprotection.

Reactions for the optimisation studies were carried out in 96-well plates in a Thermomixer (Comfort shaker (Cambridge, UK)) with constant mixing at 350 rpm and temperature control according to the setup defined by the experimental design which included: factors and their corresponding levels (Tables 1 and 2) with 2 replicates and 5 centre points. 100 μl aliquots were quenched with 100 μl of 0.2% TFA after a 24 h reaction for the recycling system, 5 h of reaction for the first two steps of the sequential cascade, and 10 h of reaction for the final transamination step of the sequential pathway. We defined the above-mentioned reaction times because in our previous work they showed full conversion (Villegas-Torres et al., 2015).

Based on the results of the optimisation, reaction profiles of the coupled reactions (Fig. 1) were performed in 5 ml glass vials in a Thermomixer (Comfort shaker (Cambridge, UK)) with constant mixing at 350 rpm and temperature control over the course of 48 h. The reaction was stopped by quenching 80 μl samples with 80 μl 0.2% TFA. The 48 h reaction allowed following the reaction performance until equilibrium of all steps in all cascades under study was reached, and determine whether the modified reaction conditions impacted the reaction time as well. In every case, prior to the addition of the enzymes, substrates were pre-incubated for 15 min at 30 °C and 350 rpm in a Thermomixer (Comfort shaker (Cambridge, UK)), and the transketolase enzyme was incubated for 20 min at room temperature with the cofactors, before it was added to the reaction mixture. All samples were analysed by HPLC. For the optimisation of the final step of the sequential pathway (Fig. 1b) glass 96-well plates were employed when methylbenzylamine (MBA) was used as amino donor.

2.4. HPLC detection

Hydroxypyruvate (HPA), pyruvate and erythrulose detection was carried out by injecting 20 μl samples into a Dionex X500 HPLC (Camberley, UK) comprising a Famos 120 autosampler, an Ultimate 3000 generation II isocratic pump, a LC30 Chromatography column oven, and an AD20 Absorbance Detector. The system was equipped with an Aminex HPX-87H Ion exchange column (300 mm × 7.8 mm, Bio-Rad, CA#1250140), run at 60 °C with 0.6 ml/ min isocratic flow of 0.1% trifluoroacetic acid (TFA) as mobile phase. Detection was performed by UV absorbance at 210 nm and peak identification and quantification were carried out using Chromeleon client 6.80 software. Commercially available standard compounds were analysed in parallel with the samples. The retention time of detected compounds are as follows: HPA: 8.3 min, Pyruvate: 9.9 min, Erythrulose: 11.5 min.

MBA, acetophenone (AP), serine and ABT were detected using a

Table 1
Summary of the optimisation factors for the recycling system, their corresponding levels and effect on reaction yield.

	FACTOR	LOW	HIGH	Model/ Transformation	Effect	*P*-value
First design space						
A	Serine concentration	50 mM	200 mM	Quadratic model/ Square		*N/S*
B	GA concentration	20 mM	100 mM	root transformation	-0.042	0.001
C	RSPH17029-3177 transaminase concentration	0.2 mg/ ml	1.0 mg/ ml	applied (P < 0.0001)	+0.31	<0.0001
D	Transketolase concentration	0.05 mg/ ml	0.5 mg/ ml		-0.084	<0.0001
E	*GA fedbatch*	0	1		-0.048	<0.0001
Interactions						
BD	GA - Transketolase concentrations				+0.055	0.0006
BE	GA concentration - Fedbatch				+0.087	<0.0001
Second design space						
A	Serine concentration	25 mM	100 mM	Quadratic model/ NT (P <	+0.37	<0.0001
B	GA concentration	10 mM	50 mM	0.0001)	+0.31	<0.0001
C	RSPH17029-3177 transaminase concentration	0.4 mg/ ml	2.0 mg/ ml		+0.75	<0.0001
D	Transketolase concentration	0.03 mg/ ml	0.25 mg/ ml		+0.17	0.0004
E	*Temperature*	15 °C	25 °C		-0.54	<0.0001
Interactions						
BD	GA – Transketolase concentration				+0.12	0.038
CD	RSPH17029-3177 transaminase – Transketolase concentration				+0.20	0.0006
CE	RSPH17029-3177 transaminase concentration – Temperature				-0.34	<0.0001
DE	Transketolase concentration – Temperature				+0.26	0.0007

N/S Factors not statistical significant (*P*-value > 0.05). *Dark grey* boxes indicate a negative effect; *light grey* boxes indicate a positive effect. Categorical variables are shown in italics.

Dionex Ultimate 3000 HPLC (Camberley, UK) with an ACE 5 C18 reverse phase column (150 mm × 4.6 mm, 5 µm particle size, Advance Chromatography Technologies, CA#CE-121-1546) controlled by Chromeleon client 6.80 software, implementing the methods reported by Ingram et al. (2007). For serine and ABT detection, 75 µl samples were derivatised prior to injection with 150 µl of 10 mg/ ml 6-Aminoquinolyl-*N*-hydroxysuccinimidyl carbamate (AQC) (Cohen and Michaud, 1993) in dry acetonitrile, followed by the addition of 225 µl of 0.2 M borate buffer pH 5. Commercially available standard compounds were analysed in parallel with the samples. ABT standard compound was synthesised as described above. The retention times of the compounds were as follows: serine: 7.3 min, ABT: 8.9 min, MBA: 3.6 min, AP: 7.6 min.

2.5. Experimental design and statistical analysis

Design Expert 8.0 software (Statease, USA) was employed for statistical experimental design. Temperature, pH and buffer type were initially tested to identify the best reaction conditions for both coupled reactions (Fig. 1), varying two buffer types at three pH values (specific for each buffer) and four different temperatures with all categorical variables (due to the software restrictions when setting up the levels to numerical variables) in a full factorial design (24 runs): Tris-HCl buffer analysed at pH 7.5, 8.0, and 9.0; and HEPES buffer at pH 7.0, 7.5, and 8.0. Both buffer types were tested at 20 °C, 25 °C, 30 °C and 37 °C.

Response Surface Methodology (RSM) using a Central Composite Design (CCD) was implemented to optimise enzymes and substrates concentrations of both cascades (Fig. 1). The recycling cascade optimisation consisted of two sets of designs: the first included 60 runs of 4 numerical factors analysed over 5 different levels, and one categorical factor with 2 levels. The second set involved 90 runs, 4 numerical variables at 5 different levels, and one categorical variable at 3 levels (Table 1). The optimisation of the sequential pathway (Fig. 1b) was performed in two phases due to the reaction limitations previously described (Villegas-Torres et al., 2015). The first phase was the optimisation of the first two sequential reactions performed by the

Table 2
Summary of the sequential pathway optimisation factors, their corresponding levels, and effect on reaction yield.

	FACTOR	LOW	HIGH	Model/ Transformation	Effect	*P*-value
First two steps						
A	Serine concentration	50 mM	200 mM	Reduced quadratic model/	+3.74	0.0001
B	GA concentration	25 mM	100 mM	NT (P < 0.0001)	+2.25	0.0136
C	Pyruvate concentration	25 mM	100 mM		+3.41	0.0004
D	DGEO0713 transaminase concentration	0.5 mg/ ml	1.0 mg/ml		+1.94	0.0311
E	Transketolase concentration	0.05 mg/ml	0.5 mg/ml			*N/S*
Interactions						
BC	GA – Pyruvate concentrations				+2.17	0.0376
Last step with MBA as amino donor						
A	Erythrulose concentration	50 mM	200 mM	Reduced quadratic model/		*N/S*
B	MBA concentration	5 mM	50 mM	NT(P < 0.0001)	-30.64	<0.0001
C	CV2025 transaminase concentration	0.3 mg/ ml	1.0 mg/ ml		+10.40	0.0258
Last step with IPA as amino donor						
A	Erythrulose concentration	50 mM	200 mM	Reduced quadratic model/	+9.52	<0.0001
B	IPA concentration	5 mM	50 mM	NT(P < 0.0001)	-19.87	<0.0001
C	CV2025 transaminase concentration	0.3 mg/ ml	1.0 mg/ ml		+15.46	<0.0001

N/S Factors not statistical significant (*P*-value > 0.05). *Dark grey* boxes indicate a negative effect; *light grey* boxes indicate a positive effect.

DGEO0713 transaminase and the transketolase. And the second corresponded to the final step of the cascade (transamination carried out by CV2025). The first two steps involved 50 runs with 5 factors varied over 5 levels, and the final step was optimised with an experimental design of 20 runs with three factors varied over 5 levels, per amino donor tested (IPA and MBA) (Table 2). ABT concentration was used as dependent variable for the recycling system (Fig. 1a). Erythrulose concentration was used as response for the first two steps of the sequential pathway (Fig. 1b), and percentage of conversion (PoC) based on limiting substrate was used as response for the final step of the sequential cascade to avoid biasing results due to variations in amino donor concentration. Fed batch reactions were performed adding half of the volume of GA at the start of the reaction, and the remaining volume 8 h later. A high concentration of GA stock solution (1 M) was employed to reduce dilution effects. Each optimisation was fitted to a specific model, and when required a transformation was applied. After model definition, data was subjected to an analysis of variance (ANOVA) to identify factor interaction and significance. Optimum values of all independent variables for the responses in each of the experimental sets were obtained using the numerical optimisation function.

3. Results

3.1. Optimisation of environmental conditions: buffer type, pH and temperature

The cascades in this study employ two transaminases recently reported (Villegas-Torres et al., 2015), for which optimum reaction conditions have not been described. Taking into account the effect of the substrates on the optimum pH stated by Shin and Kim (1999), the variability among transaminases, and the broad spectrum of buffer type, buffer concentration, pH and temperature that can be implemented in transketolase reactions, it is possible that these parameters are responsible for the low yield obtained (Villegas-Torres et al., 2015). As a result, we initially tested different buffers, pH and temperatures for each of the cascades under study.

Considering the final aim of integrating the cascades with the host metabolism, we tested a pH range from 7.0 to 9.0 since *E. coli* internal pH has been reported to be between 7.2–7.8 (Wilks and Slonczewski, 2007), using HEPES and Tris-HCl buffers as both have been employed in coupled reactions (Fotheringham et al., 1999; Iwai, 2011; Kaulmann et al., 2007; Rios-Solis et al., 2011). Phosphate buffer was not considered in spite of their extensive use (Höhne et al., 2008; Ingram et al., 2007; Koszelewski et al., 2008), because transketolase activity is negatively affected (Sprenger et al., 1995). The temperature range was evaluated between 20 °C to 37 °C and reaction time was defined as the time required to achieve full conversion (Villegas-Torres et al., 2015) since we were aiming to improve the yield.

Fig. 2 shows product concentration after 24 h of reaction for the recycling system (Fig. 2a), 5 h of reaction for the first two steps of the sequential cascade (Fig. 2b), and 10 h of reaction for the final transamination step of the sequential pathway (Fig. 2c). The last reaction step of the sequential cascade was evaluated separately from the first two steps. The recycling system had the highest product formation in 50 mM Tris-HCl buffer pH 8.0 at 25 °C (Fig. 2a). However, the yield sharply decreased at pH 9.0 compared to the other pH values tested. In addition there was a clear reduction in ABT concentration by increasing temperature above 25 °C regardless of buffer type and pH. The difference among buffer types was only significant at pH 8.0.

Previously reported, the sequential cascade (Fig. 1b) has strong side reactions that prevent it to be performed in a one-pot system (Villegas-Torres et al., 2015). Hence, the optimisation process was carried out studying the first two steps in a one-pot system and the final transamination step separately.

The first two steps of the cascade (Fig. 2b) were affected by the type of buffer as detected by the substantial difference in yield between them (10%–50% reduction). There was a clear improved conversion in HEPES buffer, which increased by increasing temperature at pH 7.0 and 7.5. At pH 8.0, the effect of temperature was negligible, synthesising the same amount of erythrulose after 5 h reaction in HEPES buffer. Therefore, the conditions that have been selected for further studies were 50 mM HEPES buffer pH 8.0 regardless of the temperature. Finally, in the case of the transamination step catalysed by the CV2025 enzyme (Fig. 2c), HEPES buffer did not affect the final conversion over the different pH values tested showing the highest conversion at pH 8.0, while with Tris-HCl buffer the yield abruptly dropped at pH 9.0. There was not a clear trend comparing the different temperatures, but at 25 °C and 37 °C the reaction achieved full conversion. Thus, to avoid HPA degradation, reported to occurred at temperatures higher than 30 °C (Rios-Solis et al., 2011), and buffer and temperature changes when coupling the whole pathway, we selected 50 mM HEPES buffer pH 8.0 at 25 °C.

3.2. Optimisation of reaction conditions: substrates and enzymes concentrations

Additional to buffer type, temperature and pH, enzymatic activity depends on substrate concentrations as they can shift the equilibrium of the reaction (Rios-Solis et al., 2011), be toxic (Chen et al., 2007) or inhibit the enzyme (Bulos and Handler, 1965; Shin and Kim, 2001, 1997). Reaction yield is also affected by enzyme concentration, the higher the concentration the higher the yield while the reaction does not reach full conversion. However, in whole cell environments there is an intrinsic limit given by the maximum enzyme expression level that can be achieved within a particular cell. As a result, we implemented enzyme and substrate concentrations as independent variables for the optimisation.

In our previous study we found that the recycling system (Fig. 1a) requires higher concentration of serine compared to GA, as well as higher concentration of transaminase than that of transketolase to synthesise ABT (Villegas-Torres et al., 2015). As a result the levels employed for substrate and enzyme concentrations are shifted (Table 1) and they only coincide in a small range in order to corroborate earlier findings. We did not employ more than 1 mg/ml per enzyme, as we noticed that above 2 mg/ml of total enzyme, within a reaction, protein aggregation occured after 5 h (data not shown). Additionally, because of the toxic effect of GA on the transketolase (Chen et al., 2006) we tested whether a GA fed-batch system would increase the overall yield.

As shown in Fig. 3a, transaminase and transketolase concentration strongly affected the reaction yield, since ABT concentration varied between 0.4 mM and 1.6 mM. RSPH17029-3177 transaminase had a positive effect, while the transketolase showed the opposite (Table 1). Thus, the highest ABT concentration was achieved at 0.8 mg/ml of RSPH17029-3177 transaminase and 0.16 mg/ml of transketolase. Serine did not affect the yield within the design space (Table 1), while GA had a negative effect (Table 1) on the reaction as expected due to its inhibitory effect on the transketolase enzyme (Chen et al., 2007). Even though, enzyme concentrations had a stronger effect (Fig. 3b) than the inhibitory substrate. Finally, the GA fed-batch process negatively affected the yield (Table 1), possibly due to a difference in substrate availability at the start of the reaction.

It is not clear whether in a different design space serine would affect the yield, and lower GA and transketolase concentration would reach a stationary point, elucidating a clear set of optimum conditions. Consequently, we performed a second optimisation study in which we decreased substrate and transketolase concentration levels and increased the transaminase concentration range (Table 1). We removed the fed batch operation, due to its negative effect, but we included temperature as categorical variable following the initial experiment to validate the prior optimisation study and tested whether there was an interaction between temperature, enzyme and substrate concentrations; that is a differential effect when varying enzyme and substrate

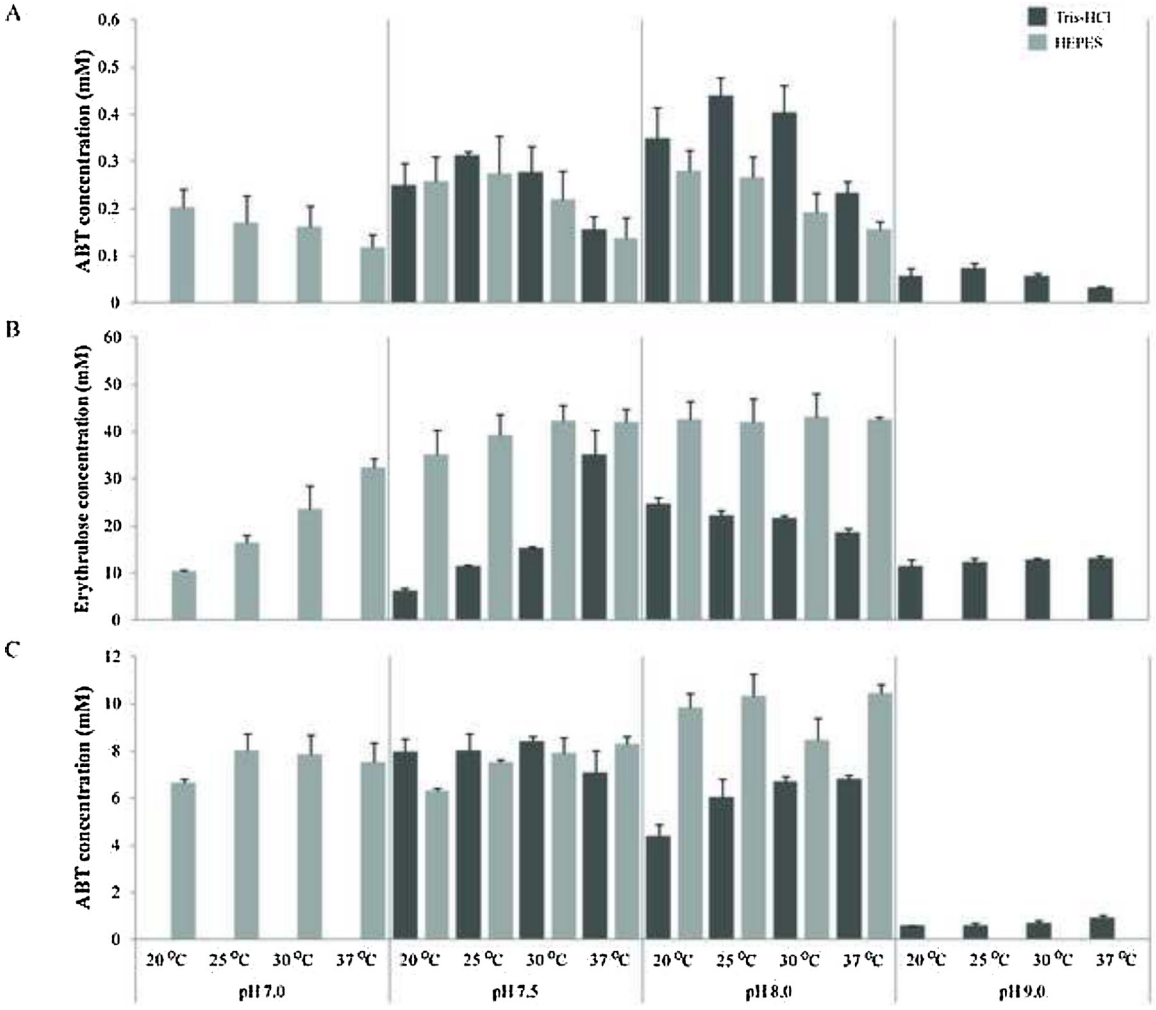

Fig. 2. Buffer type, pH and temperature optimisation for the recycling cascade (a), the first two steps of the sequential pathway (b), and the final transamination step of the sequential pathway (c). *Dark grey bars*, corresponds to the use of 50 mM Tris-HCl buffer; and *light grey bars*, to the use of 50 mM HEPES buffer. Data are the means of three independent reactions ± SE. Substrates, cofactors and enzymes concentrations were kept constant in all reactions at the following concentrations: recycling cascade: 100 mM serine, 40 mM GA, 0.9 mM $MgCl_2$, 2.4 mM TPP, 0.4 mM PLP, 1 mg/ ml RSPH17029-3177 transaminase and 0.1 mg/ ml transketolase; sequential pathway: 100 mM serine, 50 mM pyruvate, 50 mM GA, 10 mM MBA, 0.9 mM $MgCl_2$, 2.4 mM TPP, 0.4 mM PLP, 0.5 mg/ ml DGEO0713 transaminase, 0.1 mg/ ml transketolase, 0.5 mg/ ml CV2025 transaminase.

concentrations at different temperatures.

Experimental data between both optimisation studies was reproducible as similar yields were achieved over the overlapping design space between them (data not shown). Along with the first design space, the highest yield was obtained using higher transaminase concentration (Fig. 3c), while the transketolase concentration had the opposite effect (Table 1) over the evaluated range. According to the above the highest ABT yield is achieved if a transaminase/ transketolase ratio is maintained between 10 and 20. Within the second design space serine concentration showed a linear correlation with ABT concentration confirming the previous data set and indicating that concentrations above 80 mM will not significantly increase the reaction yield. Similarly, GA concentration had a positive relationship in this range (Table 1), although correlating the yield with the concentration of the limiting substrate where the highest percentage of conversion was achieved at the lowest GA concentration. The optimum temperature was 25 °C (data not shown), corroborating our previous study and supporting the strategy of testing the environmental conditions first as it reduced the number of runs without affecting the overall optimisation.

We mentioned that the sequential cascade (Fig. 1b) is strongly affected by the side reactions up to a point where ABT will not be synthesised unless both pyruvate and GA are fully consumed during the first two steps of the cascade. For that reason in our previous study we performed the reaction in a two-pot system at higher serine concentration to shift the equilibrium to the product side. In spite of the above, we only achieved a 3% conversion with this reaction scheme. According to the HPLC profile, there were some HPA and pyruvate left, which could had been the cause of the low yield (Villegas-Torres et al., 2015). Therefore in this study we employed the same pyruvate and GA concentration levels, but we kept them as individual variables in order to clarify their individual effect over the cascade. Also, serine concentration levels were set at higher values as it was shown to shift the equilibrium towards the product side (Rios-Solis et al., 2011). Alternatively, transaminase and transketolase concentration levels only had an overlapping point (transketolase upper limit and transaminase lower limit) due to the huge difference in their kinetic constants (Transketolase K_{cat}: 2442 min^{-1} (Rios-Solis et al., 2015), DGEO0713 K_{cat}: 56 min^{-1} (Villegas-Torres et al., 2015)). Thus, it is expected that small quantities of the transketolase will easily match the turnover number of the transaminase.

The first two steps of the sequential cascade (Fig. 1b) were positively affected by the substrates and the transaminase (Table 2) concentrations. Both serine and DGEO0713 concentration showed a linear

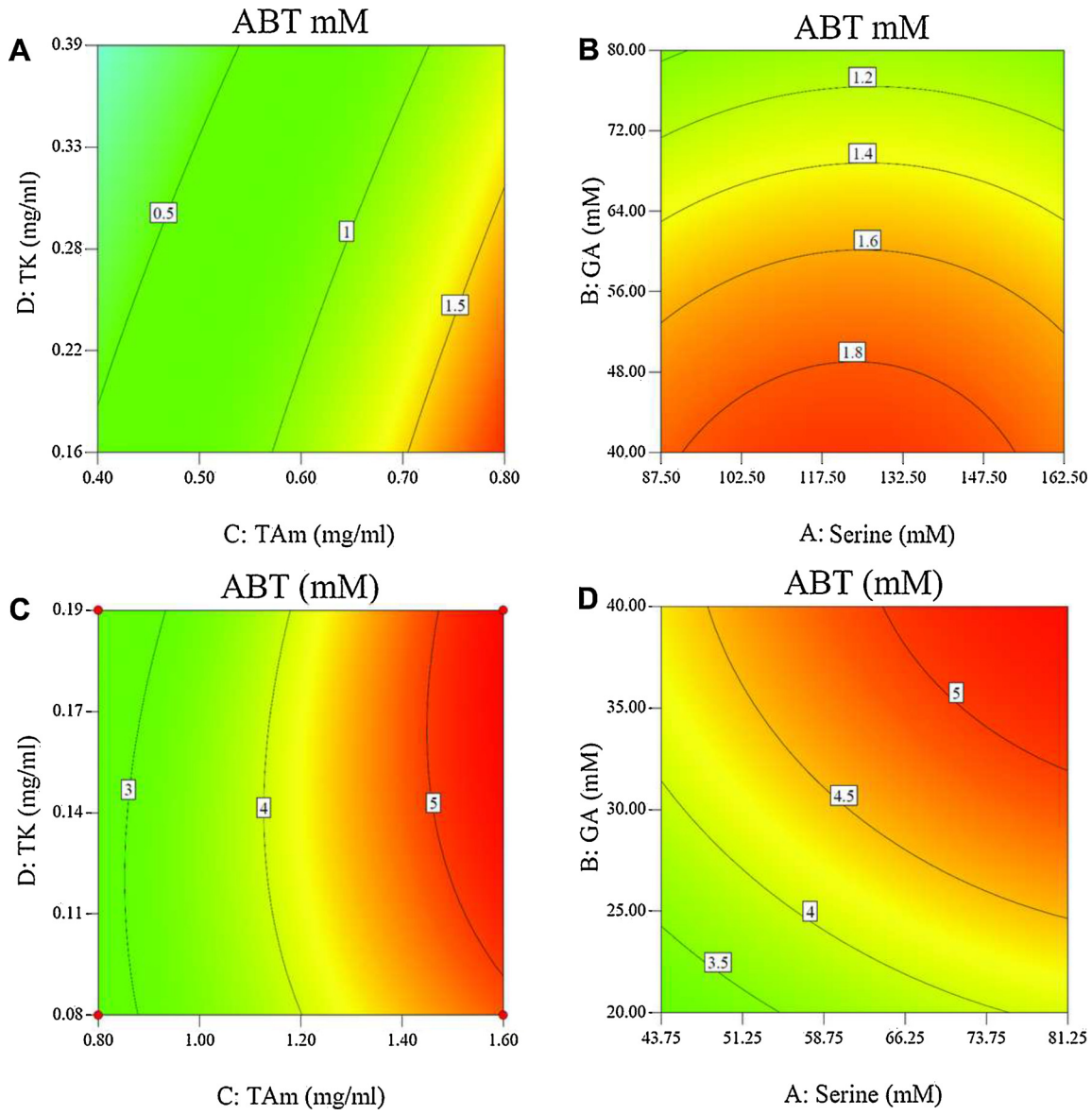

Fig. 3. Contour plots for the recycling cascade optimization. Plot for interactions between (a) RSPH17029-3177 transaminase and transketolase concentration with 126 mM serine and 40 mM GA, and (b) GA and serine concentration with 0.8 mg/ ml RSPH17029-3177 transaminase and 0.17 mg/ ml, transketolase at the first design space; and interaction plot for (c) transaminase and transketolase concentration with 80 mM serine and 40 mM GA, and (d) GA and serine concentration with 1.6 mg/ ml RSPH17029-3177 transaminase, and 0.14 mg/ ml transketolase at the second design space.

correlation with the erythrulose produced without reaching an optimum condition (Fig. 4a) compared to pyruvate and GA according to the contour plots (Fig. 4b), where 70 mM of pyruvate and 75 mM of GA gave the maximum erythrulose concentration after 24 h of reaction (Fig. 4b). When correlating the yield with the limiting substrate and taking into account the fact that both pyruvate and GA must be fully consumed only concentrations below 50 mM of the above substrates and at least 150 mM of serine resulted in 100% conversion (Fig. 4c).

The final step of the sequential system (Fig. 1b) involved the transamination of erythrulose by CV2025 transaminase. We employed percentage of conversion (PoC) as response to analyse the results due to the bias generated by low concentrations of MBA, as full conversion is expected after 24 h reaction with amino donor concentrations below 10 mM (Rios-Solis et al., 2011).

MBA concentration was the main factor negatively affecting the PoC of the second transamination (Fig. 4d) supporting the inhibitory effect previously reported (Rios-Solis et al., 2011). Transaminase concentration had a slight positive effect (Fig. 4d), while erythrulose concentration was not a significant factor (Table 2). Similarly, IPA negatively influenced the conversion, while both amino acceptor and enzyme concentrations positively affected PoC (Table 2).

3.3. Optimised reaction

As a first step towards the optimisation of the recycling cascade (Fig. 1a) and the sequential system (Fig. 1b) for their host metabolic integration we studied the influence of the environmental parameters and the reaction components on their overall yields. Based on the experimental data a statistical model was generated and employed to predict optimum conditions. The results of the predictions varied depending on the factor to be minimised: the limiting substrate or the enzyme concentration. In this study we employed purified enzymes which are 1000-times more expensive than implementing a whole cell catalyst (Tufvesson et al., 2011). Since our ultimate aim is to integrate the biocatalytic pathways with the host metabolism to carry out the synthesis in a whole cell system, the cost of the catalyst will be reduced.

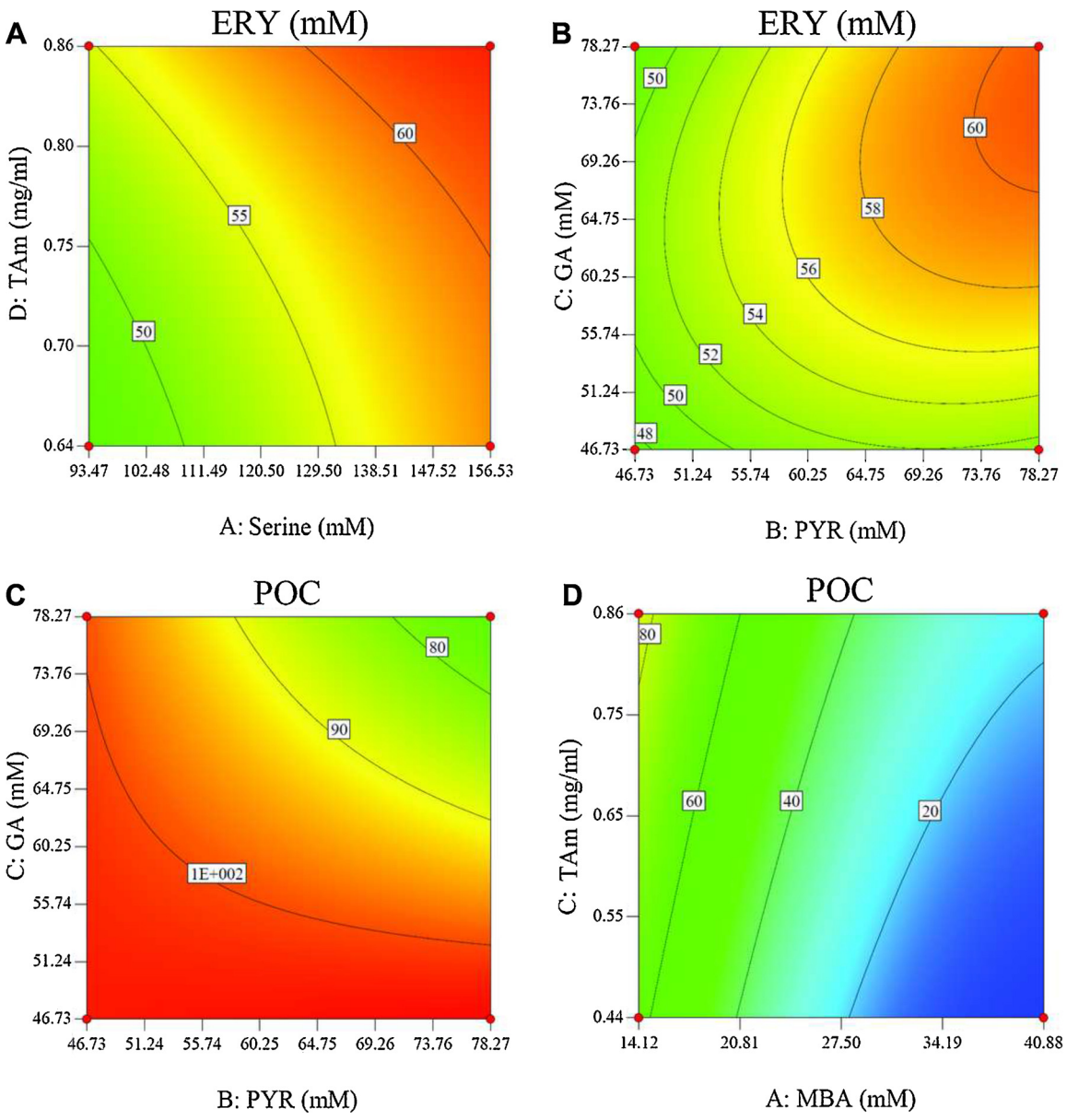

Fig. 4. Contour plots for the sequential pathway optimization. Plot for interactions between (a) serine and DGEO0713 transaminase concentrations in a reaction supplemented with 78 mM pyruvate, 78 mM GA, and 0.18 mg/ ml transketolase, and (b) pyruvate and GA concentrations for the first two steps of the cascade with 156 mM serine, 0.86 mg/ ml DGEO0713 transaminase and 0.18 mg/ ml transketolase using ABT concentration as response; interaction plot for (c) pyruvate and GA concentration with 156 mM serine, 0.86 mg/ ml DGEO0713 transaminase and 0.18 mg/ ml transketolase for the first two steps of the sequential cascade using percentage of conversion (PoC) as response; and interaction plot for (d) MBA and CV2025 transaminase concentrations using 170 mM erythrulose for the final step of the pathway.

Therefore, we decided that the optimisation should maximise product concentration at the minimum substrate concentration possible. Implementing the above restrictions optimum conditions suggested were as following; for the recycled cascade: 80 mM serine, 40 mM GA, 0.15 mg/ml transketolase and 2.0 mg/ml RSPH17029-3177 transaminase; and for the sequential pathway: 150 mM serine, 50 mM pyruvate, 50 mM GA, 5 mM MBA, 0.5 mg/ml transketolase, 0.5 mg/ ml DGEO0713 transaminase, and 1 mg/ml CV2025 transaminase.

Fig. 5a shows the reaction profile of the recycling system based on the results of the numerical optimisation. After 48 h reaction the PoC previously achieved (Villegas-Torres et al., 2015) was doubled, obtaining more than 5 mM of ABT synthesised. The mass balance could not be determined because GA and ethanolamine (side reaction product of GA transamination with serine) were not detected. However, after 4 h of reaction maximum erythrulose concentration is achieved (based on initial substrate concentration) indicating that the glycolaldehyde had been fully consumed. Consequently, HPA concentration levelled off at that point. Overall, 60% conversion based on the glyceraldehyde available for the erythrulose-producing reaction was achieved, resulting in 2-fold improvement compared to our earlier work.

The first two steps of the sequential cascade were optimised to achieve full conversion before the third step was initiated. After 24 h reaction (Fig. 5b) all pyruvate was consumed synthesising 50 mM erythrulose, suggesting that all GA was depleted. When adding the third enzyme (CV2025 transaminase, dotted line in Fig. 5b) erythrulose concentration was diluted, thus MBA concentration was proportionally reduced. After 24 h, only 10% conversion was reached. A 3-times improvement was achieved compared to the proof of concept (Villegas-Torres et al., 2015) but the expected full conversion was not attained. This cannot be attributed to pH changes as it was controlled before the

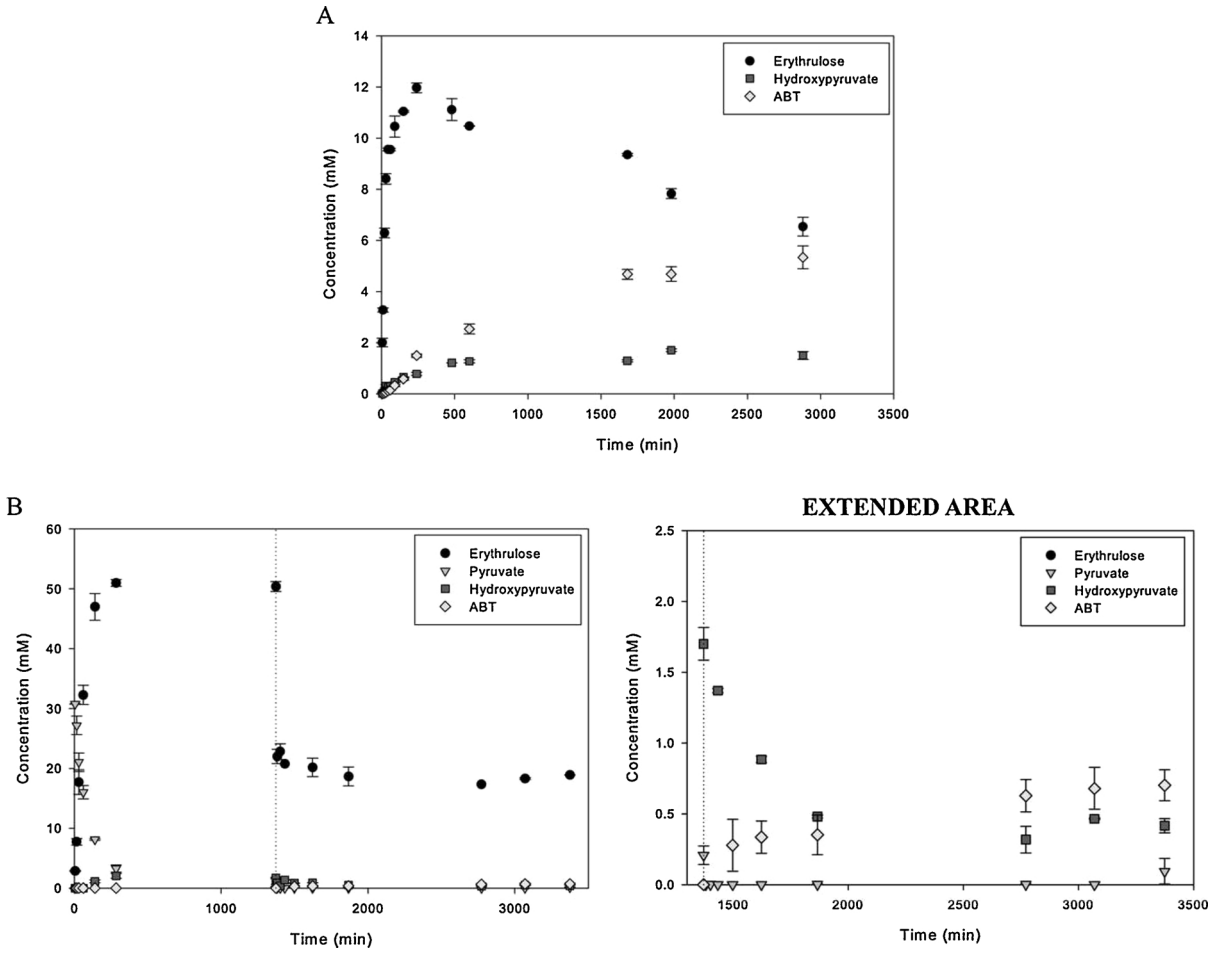

Fig. 5. Reaction profiles for the synthesis of ABT using (a) the recycling cascade, and (b) the sequential pathway. *Dotted line* corresponds to the addition of CV2025 transaminase. The area after the dotted line is extended next to the graph. Reactions were carried out according to the optimization results for each scheme (Recycling cascade: performed in Tris-HCl pH 8.0 at 25 °C, with 80 mM serine, 40 mM GA, 0.15 mg/ ml transketolase and 2.0 mg/ ml RSPH17029-3177 transaminase. Sequential pathway: carried out in HEPES pH 8.0 at 30 °C initially, and then dropped to 25 °C for the last step, with 150 mM serine, 50 mM pyruvate, 50 mM GA, 5 mM MBA, 0.5 mg/ ml transketolase, 0.5 mg/ ml DGEO0713 transaminase, and 1 mg/ml CV2025 transaminase). Erythrulose, *black* circles; pyruvate, *grey inverse triangle*; HPA, *dark grey square*; and ABT, *light grey diamond*, were measured over time for 48 h and quantified by HPLC. Data are the means of three independent reactions ± SE.

final enzymatic step took place, neither to side reactions with pyruvate and GA because their full consumption was ensured by HPLC analysis (Fig.5b) before the final step was initiated. The other components within the system besides the added MBA and the produced erythrulose were alanine, and the enzymes from the first two steps. Alanine has been previously used as amino donor (Bulos and Handler, 1965; Shin and Kim, 2001; Wilding et al., 2016) and the transketolase enzyme was present in previous studies where CV2025 transaminase was used in a two-pot system (Rios-Solis et al., 2011), thus inhibition from these components is not expected. Consequently we tested whether the DGEO0713 transaminase negatively affect the CV2025 transaminase by adding the first enzyme into the reaction performed by the second transaminase. We also determined the second transamination yield after removing the precipitate from the first two steps of the sequential pathway. DGEO0713 transaminase on its own did not inhibit CV2025 transaminase reaction and the precipitate removal did not increase the yield (data not shown). To further increase ABT concentration by the sequential pathway reaction process engineering must be implemented, which is beyond the scope of this work (Fig. 1B).

4. Discussion

RSM has been widely implemented for the optimisation of single step biocatalytic processes (Hari Krishna et al., 2000; Zhang et al., 2016) and recently of cascades (Bornadel et al., 2016; Babaki et al., 2017) as it identifies both individual and combinatorial effects from a set of independent variables generating a mathematical model (Andersson and Adlercreutz, 1999; Baş and Boyacı, 2007). We successfully implemented it for the optimisation of two different multistep biocatalytic approaches: a recycling cascade (Fig. 1a) and a sequential pathway (Fig. 1b), resulting in a 2-fold and 3-fold improvement, respectively. The use of RSM reduced the experimental effort and time required if kinetic modelling would have been employed. For example Rios-Solis and collaborators carried out at least 54 reactions, sampling multiple times each reaction and analysing at least 252 samples by HPLC (Rios-Solis et al., 2013) to develop the kinetic model of a 2-enzyme cascade. In this work we performed a total of 220 reactions sampled individually only once, thus analysing equal number of HPLC samples for the optimisation of two different pathways: one with two enzymes and the other with three enzymes. However, the depth of information was compromised as specific data such as toxicity, stability and inhibition constants cannot be determined with the experimental design used. Instead, we focussed on the higher conversion and thereby obtained a general understanding of the effects from the individual variables, as well as their interaction in each coupled reaction.

The recycling cascade (Fig. 1b) was previously reported as an

attractive approach for the synthesis of ABT and its integration with the host metabolism, but higher yields and better system understanding was required (Villegas-Torres et al., 2015). Contrasting the effect of the variables at each design space evaluated (Table 2), in the second design space, where substrates are studied at lower concentrations and enzymes at higher level, all factors had stronger positive effects. The above is a clear indication of substrate inhibition, which in this cascade is caused by GA as serine either exerts a positive effect or none. On the other hand, the results suggested that a transaminase/transketolase ratio between 10 and 20 is required to achieve the highest yield detected. This result agrees with the transketolase/transaminase ratio reported by Rios-Solis and collaborators (Rios-Solis et al., 2015), where they projected a similar ratio assuming equimolar concentrations based on modelling predictions. In this case, the defined transaminase/transketolase ratio is based on experimental data where external effects are taking into account increasing the certainty of the result.

In our previous study (Villegas-Torres et al., 2015) we characterised a serine:pyruvate transaminase, which we coupled to the previously described *de novo* pathway employed for the synthesis of ABT (Ingram et al., 2007; Rios-Solis et al., 2011) corresponding to the reaction scheme in Fig. 1b. According to our results, the strong side reactions catalysed by the ω-transaminase (CV2025) affected the overall conversion. In this work, we implemented RSM for its optimisation in order to fully consume the substrates prior to the final enzymatic step. The experimental data indicated an interaction between pyruvate and GA concentration, which was expected due to the direct dependency of both substrates for erythrulose synthesis. The first two steps were affected only by the transaminase concentration due to the large difference in turnover number between the transamination and the transketolase reaction (Villegas-Torres et al., 2015). In spite of the successful optimisation of the first two steps, we could not reach high conversion levels (10%), even though 87% conversion has been reported for the final two steps (Rios-Solis et al., 2011). Substrates from the first two steps were fully consumed except serine, which was added in excess to shift the equilibrium towards the product side (trend supported by our data). Serine can act as amino donor as well as alanine (a side product of the first reaction) in the synthesis of ABT from erythrulose, thus the low conversion cannot be attributed to side reactions. A negative interaction between the transaminases, and a loss of enzyme activity by the purification processes were also ruled out. For that reason, further studies are required to understand the negative effect exerted by the first transamination reaction over the transketolase/transaminase pathway previously described (Smith et al., 2010).

One of the disadvantages of using transaminases for the synthesis of chiral amino alcohols is their low equilibrium constant (Shin and Kim, 2001). Several strategies have been applied to shift the reaction equilibrium (Shin and Kim, 1997; Shin et al., 2001), including the implementation of coupled reactions (Ingram et al., 2007; Koszelewski et al., 2011; Rios-Solis et al., 2011; Tauber et al., 2013). In this work, the recycling cascade (Fig. 1a) designed to remove and synthesise the amino acceptor for both reactions involved in the pathway, required a small supplement of the transketolase substrate, namely HPA, to initiate the cascade. A side reaction carried out by the same ω-transaminase, using serine and GA as substrates, consumed more than the 50% of the GA available (Villegas-Torres et al., 2015). After optimising the system the equilibrium was shifted to 60% (taking into account GA consumption by the side reaction). This conversion agrees with an approach in which a simultaneous recycling mechanism is implemented for cofactor and amino donor (Tauber et al., 2013). In spite of the similar equilibrium between the above cascades, Tauber et al. (2013) shifted the equilibrium even further (up to 90%) by using the enzymes in lysate form. In our case, the equilibrium is dependent on the transaminase activity towards GA as this enzyme prefers this amino acceptor to erythrulose consuming it entirely early in the reaction. This causes the accumulation of HPA restricting a further shift in the reaction equilibrium. The implementation of protein engineering to improve enzyme activity towards erythrulose and decrease it towards GA could benefit the overall conversion. Regarding the sequential pathway, the first two steps achieved full conversion due to the irreversible characteristic of the transketolase reaction by producing carbon dioxide when HPA is the carbon donor. However, the final step of the reaction reached equilibrium at very low conversion regardless of higher erythrulose concentration, which in a previous study was enough to shift the equilibrium up to 90% to the product side (Rios-Solis et al., 2011). Therefore, further studies are required to increase final yields of the sequential pathway.

5. Conclusion

As concluding remarks, we employed RSM to optimise the conversion of two different reaction cascades for the synthesis of ABT. The first corresponded to a recycling cascade (Fig. 1a), which led to a 2-fold improvement. According to the results, this system strongly depends on the transaminase step and is inhibited by GA. Additionally we determined that a ratio of transaminase to transketolase between 10 and 20 to 1 is ideal for the highest conversion, which should be taken into account when defining the regulatory mechanisms for enzyme expression in a whole cell system. For the second cascade, a sequential 3-step pathway (Fig. 1b), the overall conversion improved 3-times after the optimisation study. This system reached 100% conversion after the first two steps, but the limiting reaction was the final transamination by CV2025, which resulted in only 10% conversion. Therefore, the methodology implemented here allows increasing final yields and helping to identify bottlenecks and limitations in *de novo* pathways. The above is possible with reduced experimental effort, while compromising in-depth kinetic analysis; thus it is a useful approach for optimising reaction conditions and defining the relative enzyme expression levels in multi-step reactions.

Acknowledgements

The authors would like to thank the UK Engineering and Physical Sciences Research Council (EPSRC) for support of the multidisciplinary Bioconversion Integrated with Chemistry and Engineering (BiCE) programme (GR/S62505/01). Support to M.F.V.T by COLFUTURO and COLCIENCIAS is also acknowledged.

References

Andersson, M., Adlercreutz, P., 1999. Evaluation of simple enzyme kinetics by response surface modelling. Biotechnol. Tech. 13, 903–907. https://doi.org/10.1023/A:1008994613645.

Babaki, M., Yousefi, M., Habibi, Z., Mohammadi, M., 2017. Process optimization for biodiesel production from waste cooking oil using multi-enzyme systems through response surface methodology. Renew. Energy 105, 465–472. https://doi.org/10.1016/j.renene.2016.12.086.

Baş, D., Boyacı, İ.H., 2007. Modeling and optimization I: usability of response surface methodology. J. Food Eng. 78, 836–845. https://doi.org/10.1016/j.jfoodeng.2005.11.024.

Beg, Q.K., Saxena, R.K., Gupta, R., 2002. Kinetic constants determination for an alkaline protease from Bacillus mojavensis using response surface methodology. Biotechnol. Bioeng. 78, 289–295. https://doi.org/10.1002/bit.10203.

Bongs, J., Hahn, D., Schörken, U., Sprenger, G.A., Kragl, U., Wandrey, C., 1997. Continuous production of erythrulose using transketolase in a membrane reactor. Biotechnol. Lett. 19, 213–216. https://doi.org/10.1023/A:1018341204341.

Bornadel, A., Hatti-Kaul, R., Hollmann, F., Kara, S., 2016. Enhancing the productivity of the bi-enzymatic convergent cascade for ε-caprolactone synthesis through design of experiments and a biphasic system. Tetrahedron 72, 7222–7228. https://doi.org/10.1016/j.tet.2015.11.054.

Bradford, M.M., 1976. A rapid and sensitive method for the quantitation of microgram quantities of protein utilizing the principle of protein-dye binding. Anal. Biochem. 72, 248–254. https://doi.org/10.1016/0003-2697(76)90527-3.

Brocklebank, S., Woodley, J.M., Lilly, M.D., 1999. Immobilised transketolase for carbon-carbon bond synthesis: biocatalyst stability. J. Mol. Catal. B Enzym. 7, 223–231. https://doi.org/10.1016/S1381-1177(99)00031-4.

Bulos, B., Handler, P., 1965. Kinetics of beef heart glutamic-alanine transaminase. J. Biol. Chem. 240, 3283–3294.

Cázares, A., Galman, J.L., Crago, L.G., Smith, M.E.B., Strafford, J., Ríos-Solís, L., Lye, G.J.,

Dalby, P.A., Hailes, H.C., 2010. Non-α-hydroxylated aldehydes with evolved transketolase enzymes. Org. Biomol. Chem. 8, 1301. https://doi.org/10.1039/b924144b.
Chen, B.H., Sayar, A., Kaulmann, U., Dalby, P.A., Ward, J.M., Woodley, J.M., 2006. Reaction modelling and simulation to assess the integrated use of transketolase and ω-transaminase for the synthesis of an aminotriol. Biocatal. Biotransform. 24, 449–457. https://doi.org/10.1080/10242420601068668.
Chen, B.H., Baganz, F., Woodley, J.M., 2007. Modelling and optimisation of a transketolase-mediated carbon-carbon bond formation reaction. Chem. Eng. Sci. 62, 3178–3184. https://doi.org/10.1016/j.ces.2007.02.025.
Cohen, S.A., Michaud, D.P., 1993. Synthesis of a fluorescent derivatizing reagent, 6-aminoquinolyl-N-hydroxysuccinimidyl carbamate, and its application for the analysis of hydrolysate amino acids via high-performance liquid chromatography. Anal. Biochem. 211, 279–287. https://doi.org/10.1006/abio.1993.1270.
Contestabile, R., John, R.A., 1996. The mechanism of high-yielding chiral syntheses catalysed by wild-type and mutant forms of aspartate aminotransferase. Eur. J. Biochem. 240, 150–155. https://doi.org/10.1111/j.1432-1033.1996.0150h.x.
Costelloe, S.J., Ward, J.M., Dalby, P.A., 2007. Evolutionary analysis of the TPP-dependent enzyme family. J. Mol. Evol. 66, 36–49. https://doi.org/10.1007/s00239-007-9056-2.
Dequeker, E., Compernolle, F., Toppet, S., Hoornaert, G., 1995. Diastereoselective conversion of L-(S)-erythrulose to 2-amino-2-deoxy-L-erythritol. Tetrahedron 51, 5877–5890. https://doi.org/10.1016/0040-4020(95)00239-5.
Erb, T.J., Jones, P.R., Bar-Even, A., 2017. Synthetic metabolism: metabolic engineering meets enzyme design. Curr. Opin. Chem. Biol. 37, 56–62. https://doi.org/10.1016/j.cbpa.2016.12.023.
Fang, H., Dong, H., Cai, T., Zheng, P., Li, H., Zhang, D., Sun, J., 2016. In vitro optimization of enzymes involved in precorrin-2 synthesis using response surface methodology. PLoS One 11, e0151149. https://doi.org/10.1371/journal.pone.0151149.
Fotheringham, I.G., Grinter, N., Pantaleone, D.P., Senkpeil, R.F., Taylor, P.P., 1999. Engineering of a novel biochemical pathway for the biosynthesis of -2-aminobutyric acid in Escherichia coli K12. Bioorg. Med. Chem. 7, 2209–2213. https://doi.org/10.1016/S0968-0896(99)00153-4.
Gyamerah, M., Willetts, A.J., 1997. Kinetics of overexpressed transketolase from Escherichia coli JM 107/pQR 700. Enzyme Microb. Technol. 20, 127–134. https://doi.org/10.1016/S0141-0229(96)00106-8.
Hanai, T., Atsumi, S., Liao, J.C., 2007. Engineered synthetic pathway for isopropanol production in Escherichia coli. Appl. Environ. Microbiol. 73, 7814–7818. https://doi.org/10.1128/AEM.01140-07.
Hari Krishna, S., Manohar, B., Divakar, S., Prapulla, S.G., Karanth, N.G., 2000. Optimization of isoamyl acetate production by using immobilized lipase from mucor miehei by response surface methodology. Enzyme Microb. Technol. 26, 131–136. https://doi.org/10.1016/S0141-0229(99)00149-0.
Hibbert, E.G., Senussi, T., Costelloe, S.J., Lei, W., Smith, M.E.B., Ward, J.M., Hailes, H.C., Dalby, P.A., 2007. Directed evolution of transketolase activity on non-phosphorylated substrates. J. Biotechnol. 131, 425–432. https://doi.org/10.1016/j.jbiotec.2007.07.949.
Hibbert, E.G., Senussi, T., Smith, M.E.B., Costelloe, S.J., Ward, J.M., Hailes, H.C., Dalby, P.A., 2008. Directed evolution of transketolase substrate specificity towards an aliphatic aldehyde. J. Biotechnol. 134, 240–245. https://doi.org/10.1016/j.jbiotec.2008.01.018.
Höhne, M., Kühl, S., Robins, K., Bornscheuer, U.T., 2008. Efficient asymmetric synthesis of chiral amines by combining transaminase and pyruvate decarboxylase. Chembiochem: Eur. J. Chem. Biol. 9, 363–365. https://doi.org/10.1002/cbic.200700601.
Ingram, C., Bommer, M., Smith, M., Dalby, P., Ward, J., Hailes, H., Lye, G., 2007. One-pot synthesis of amino-alcohols using a de-novo transketolase and beta-alanine: pyruvate transaminase pathway in Escherichia coli. Biotechnol. Bioeng. 96, 559–569. https://doi.org/10.1002/bit.21125.
Iwai, N., 2011. One-pot three-step continuous enzymatic synthesis of 5-fluoro-5-deoxy-d-ribose. J. Mol. Catal., B Enzym. 73, 1–4.
Kaulmann, U., Smithies, K., Smith, M.E.B., Hailes, H.C., Ward, J.M., 2007. Substrate spectrum of omega-transaminase from Chromobacterium violaceum DSM30191 and its potential for biocatalysis. Enzyme Microb. Technol. 41, 628–637. https://doi.org/10.1016/j.enzmictec.2007.05.011.
Kim, K.H., 1964. Purification and properties of a diamine alpha-ketoglutarate transaminase from Escherichia coli. J. Biol. Chem. 239, 783–786.
Koszelewski, D., Lavandera, I., Clay, D., Rozzell, D., Kroutil, W., 2008. Asymmetric synthesis of optically pure pharmacologically relevant amines employing omega-transaminases. Adv. Synth. Catal. 350, 2761–2766. https://doi.org/10.1002/adsc.200800496.
Koszelewski, D., Grischek, B., Glueck, S.M., Kroutil, W., Faber, K., 2011. Enzymatic racemization of amines catalyzed by enantiocomplementary ω-transaminases. Chem. – Eur. J. 17, 378–383. https://doi.org/10.1002/chem.201001602.
Martinez-Torres, R.J., Aucamp, J.P., George, R., Dalby, P.A., 2007. Structural stability of E. coli transketolase to urea denaturation. Enzyme Microb. Technol. 41, 653–662. https://doi.org/10.1016/j.enzmictec.2007.05.019.
Mitra, R.K., Woodley, J.M., Lilly, M.D., 1998. Escherichia coli transketolase-catalyzed carbon-carbon bond formation: biotransformation characterization for reactor evaluation and selection. Enzyme Microb. Technol. 22, 64–70. https://doi.org/10.1016/S0141-0229(97)00106-3.
Morales, M., Ataman, M., Badr, S., Linster, S., Kourlimpinis, I., Papadokonstantakis, S., Hatzimanikatis, V., Hungerbühler, K., 2016. Sustainability assessment of succinic acid production technologies from biomass using metabolic engineering. Energy Environ. Sci. 9, 2794–2805. https://doi.org/10.1039/C6EE00634E.
Niu, W., Molefe, M.N., Frost, J.W., 2003. Microbial synthesis of the energetic material precursor 1,2,4-butanetriol. J. Am. Chem. Soc. 125, 12998–12999. https://doi.org/10.1021/ja036391+.
Prather, K., Martin, C., 2008. De novo biosynthetic pathways: rational design of microbial chemical factories. Curr. Opin. Biotechnol. 19, 468–474. https://doi.org/10.1016/j.copbio.2008.07.009.
Rios-Solis, L., Halim, M., Cázares, A., Morris, P., Ward, J.M., Hailes, H.C., Dalby, P.A., Baganz, F., Lye, G.J., 2011. A toolbox approach for the rapid evaluation of multi-step enzymatic syntheses comprising a “mix and match” E. coli expression system with microscale experimentation. Biocatal. Biotransform. 29, 192–203. https://doi.org/10.3109/10242422.2011.609589.
Rios-Solis, L., Bayir, N., Halim, M., Du, C., Ward, J.M., Baganz, F., Lye, G.J., 2013. Non-linear kinetic modelling of reversible bioconversions: application to the transaminase catalyzed synthesis of chiral amino-alcohols. Biochem. Eng. J. 73, 38–48. https://doi.org/10.1016/j.bej.2013.01.010.
Rios-Solis, L., Morris, P., Grant, C., Odeleye, A.O.O., Hailes, H.C., Ward, J.M., Dalby, P.A., Baganz, F., Lye, G.J., 2015. Modelling and optimisation of the one-pot, multi-enzymatic synthesis of chiral amino-alcohols based on microscale kinetic parameter determination. Chem. Eng. Sci. 122, 360–372. https://doi.org/10.1016/j.ces.2014.09.046.
Shin, J.S., Kim, B.G., 1997. Kinetic resolution of alpha-methylbenzylamine with omicron-transaminase screened from soil microorganisms: application of a biphasic system to overcome product inhibition. Biotechnol. Bioeng. 55, 348–358. https://doi.org/10.1002/(SICI)1097-0290(19970720)55:2<348::AID-BIT12>3.0.CO;2-D.
Shin, J.S., Kim, B.G., 1999. Asymmetric synthesis of chiral amines with omega-transaminase. Biotechnol. Bioeng. 65, 206–211.
Shin, J.S., Kim, B.G., 2001. Comparison of the omega-transaminases from different microorganisms and application to production of chiral amines. Biosci. Biotechnol. Biochem. 65, 1782–1788.
Shin, J.-S., Kim, B.-G., Liese, A., Wandrey, C., 2001. Kinetic resolution of chiral amines with omega-transaminase using an enzyme-membrane reactor. Biotechnol. Bioeng. 73, 179–187. https://doi.org/10.1002/bit.1050.
Smith, M., Chen, B., Hibbert, E., Kaulmann, U., Smithies, K., Galman, J., Baganz, F., Lye, G., Ward, J., Woodley, J., Micheletti, M., 2010. A multidisciplinary approach toward the rapid and preparative-scale biocatalytic synthesis of chiral amino alcohols: a concise transketolase-omega-transaminase-mediated synthesis of (2S,3S)-2-amino-pentane-1,3-diol. Org. Process Res. Dev. 14, 99–107. https://doi.org/10.1021/op900190y.
Sprenger, G.A., Schörken, U., Sprenger, G., Sahm, H., 1995. Transketolase A of Escherichia coli K12. Purification and properties of the enzyme from recombinant strains. Eur. J. Biochem. FEBS 230, 525–532.
Tauber, K., Fuchs, M., Sattler, J.H., Pitzer, J., Pressnitz, D., Koszelewski, D., Faber, K., Pfeffer, J., Haas, T., Kroutil, W., 2013. Artificial multi-enzyme networks for the asymmetric amination of sec-alcohols. Chem. Weinh. Bergstr. Ger. 19, 4030–4035. https://doi.org/10.1002/chem.201202666.
Tufvesson, P., Lima-Ramos, J., Nordblad, M., Woodley, J.M., 2011. Guidelines and cost analysis for catalyst production in biocatalytic processes. Org. Process Res. Dev. 15, 266–274. https://doi.org/10.1021/op1002165.
Vasic-Racki, D., Kragl, U., Liese, A., 2003. Benefits of enzyme kinetics modelling. Chem. Biochem. Eng. Q. 17, 7–18.
Villegas-Torres, M.F., Martinez-Torres, R.J., Cázares-Körner, A., Hailes, H., Baganz, F., Ward, J., 2015. Multi-step biocatalytic strategies for chiral amino alcohol synthesis. Enzyme Microb. Technol. 81, 23–30. https://doi.org/10.1016/j.enzmictec.2015.07.003.
Wilding, M., Peat, T.S., Newman, J., Scott, C., 2016. A β-alanine catabolic pathway containing a highly promiscuous ω-transaminase from the 12-aminododecanate-degrading Pseudomonas sp. Strain AAC. Appl. Environ. Microbiol. AEM 82, 3846–3856. https://doi.org/10.1128/AEM.00665-16.
Wilks, J.C., Slonczewski, J.L., 2007. pH of the cytoplasm and periplasm of Escherichia coli: rapid measurement by green fluorescent protein fluorimetry. J. Bacteriol. 189, 5601–5607. https://doi.org/10.1128/JB.00615-07.
Yamamoto, K., Kataoka, E., Miyamoto, N., Furukawa, K., Ohsuye, K., Yabuta, M., 2003. Genetic engineering of Escherichia coli for production of tetrahydrobiopterin. Metab. Eng. 5, 246–254. https://doi.org/10.1016/S1096-7176(03)00046-6.
Yang, Y.-T., Bennett, G.N., San, K.-Y., 1998. Genetic and metabolic engineering. Electron. J. Biotechnol. 1, 134–141. https://doi.org/10.2225/vol1-issue3-fulltext-3.
Yonaha, K., Toyama, S., 1980. gamma-aminobutyrate:alpha-ketoglutarate aminotransferase from pseudomonas sp. F-126: purification, crystallization, and enzymologic properties. Arch. Biochem. Biophys. 200, 156–164.
Zhang, D.-H., Zhang, J.-Y., Che, W.-C., Wang, Y., 2016. A new approach to synthesis of benzyl cinnamate: optimization by response surface methodology. Food Chem. 206, 44–49. https://doi.org/10.1016/j.foodchem.2016.03.015.